Research

Check for updates

Author for correspondence:
I. G. Nizovtseva
e-mail: nizovtseva.irina@gmail.com

Travelling-wave amplitudes as solutions of the phase-field crystal equation

I. G. Nizovtseva[1,2] and P. K. Galenko[1,2]

[1]Department of Theoretical and Mathematical Physics, Laboratory of Multi-Scale Mathematical Modeling, Ural Federal University, Ekaterinburg, 620000, Russian Federation
[2]Physikalisch-Astronomische Fakultät, Friedrich-Schiller-Universität Jena, 07743 Jena, Germany

IGN, 0000-0002-7766-7351; PKG, 0000-0003-2941-7742

The dynamics of the diffuse interface between liquid and solid states is analysed. The diffuse interface is considered as an envelope of atomic density amplitudes as predicted by the phase-field crystal model (Elder *et al.* 2004 *Phys. Rev. E* **70**, 051605 (doi:10.1103/PhysRevE.70.051605); Elder *et al.* 2007 *Phys. Rev. B* **75**, 064107 (doi:10.1103/PhysRevB.75.064107)). The propagation of crystalline amplitudes into metastable liquid is described by the hyperbolic equation of an extended Allen–Cahn type (Galenko & Jou 2005 *Phys. Rev. E* **71**, 046125 (doi:10.1103/PhysRevE.71.046125)) for which the complete set of analytical travelling-wave solutions is obtained by the tanh method (Malfliet & Hereman 1996 *Phys. Scr.* **15**, 563–568 (doi:10.1088/0031-8949/54/6/003); Wazwaz 2004 *Appl. Math. Comput.* **154**, 713–723 (doi:10.1016/S0096-3003(03)00745-8)). The general tanh solution of travelling waves is based on the function of hyperbolic tangent. Together with its set of particular solutions, the general tanh solution is analysed within an example of specific task about the crystal front invading metastable liquid (Galenko *et al.* 2015 *Phys. D* **308**, 1–10 (doi:10.1016/j.physd.2015.06.002)). The influence of the driving force on the phase-field profile, amplitude velocity and correlation length is investigated for various relaxation times of the gradient flow.

This article is part of the theme issue 'From atomistic interfaces to dendritic patterns'.

1. Introduction

The phase-field crystal (PFC) model has been used to examine the dynamics of liquid–solid transformation, grain boundary migration and dislocation motion [1–3]. The PFC model is a continuum model that describes processes on atomic length scales and pattern on the nano- and micro-length scales [4]. This model is characterized by a free energy which is represented by a functional of a conserved atomic density field that is periodic in the solid phase and uniform in a liquid state. One of the simplest ways to analyse the PFC model is to use the amplitude equations [5–7] which represent smooth profiles over peaks of the density field (see a short discussion about obtaining the amplitude equation of the PFC equation in appendix A). Taking into account slow and fast degrees of freedom for the crystal–liquid interface propagation, the amplitude equation of the PFC model is described by the following partial differential equation (PDE) [8]:

$$\tau \frac{\partial^2 u}{\partial t^2} + \frac{\partial u}{\partial t} = \nabla^2 u - K_0 u + b u^2 - u^3. \tag{1.1}$$

The following notations are introduced in equation (1.1): $u(\mathbf{r}, t)$ is the amplitude of atomic density (order parameter), τ is the time for relaxation of the rate $\partial u/\partial t$, i.e. the gradient flow (τ has a real value smaller than the relaxation time of the amplitude u as defined in [8]), $\mathbf{r}$ is the radius vector, t is the time, and the parameter b is given by

$$b = \frac{2a}{\sqrt{15v|\Delta B_0|}}, \tag{1.2}$$

where the driving force ΔB_0 describes

$$\Delta B_0 = \begin{cases} \Delta B_0 > 0, & \text{the transition from a metastable state with } K_0 = +1, \\ \Delta B_0 < 0, & \text{the transition from an unstable state with } K_0 = -1, \end{cases} \tag{1.3}$$

a and v are the coefficients in the free energy, which has the form of Landau–de Gennes potential:

$$f(u) = \frac{K_0 \Delta B_0}{2} u^2 - \frac{2a}{3} u^3 + \frac{15v}{4} u^4. \tag{1.4}$$

As it follows from equation (1.4), the two states (liquid and solid) have equal energy in the equilibrium with the parameter $b = 8a^2/135v$ and the crystalline front has zero velocity.

Equation (1.1) can be considered as an extended Cahn–Allen equation which transforms to its standard form at $b = 0$ and $\tau = 0$ [9], which was suggested for the anti-phase boundary motion and then used in a wide spectrum of mathematical and physical applications [10], for instance, in description of free-boundary problems by the phase-field method [4]. In its complete form, equation (1.1) has been applied in the field of fast-phase transitions [11,12] whose validity has been verified by comparison with experimental data [13], in molecular dynamics simulations [14] and by coarse-graining derivations of the phase-field equations [15].

PDE can be analysed using an important class of travelling-wave solutions which, in their particular form, include tanh functions [16,17]. Particular solutions of equation (1.1) have also been found in the form of tanh function [8]. However, there exists no general set of travelling waves for the hyperbolic equation of Allen–Cahn type (1.1). Therefore, the main purpose of the present work is to find a complete set of travelling waves for equation (1.1). This set will be found using the tanh method [16–19] representing one of the ways of searching for solutions of travelling waves (as one of the applications of this method to physically relevant tasks, one can mention the work of Kourakis *et al.* [20]). The complete set of solutions will be checked on the existence of tanh functions.

2. Travelling waves by the tanh method

One of the important solutions for the analysis of phase transformations is related to travelling waves [8,10,16–19,21]. To treat the nonlinear PDEs, the travelling waves are obtained by the

first integral method [21–24] (which can be considered as one of particular cases of the direct method [25], generalizing the use of equivalent methods of finding the exact solutions of PDE, which were reduced to ODE [26]), and also using the G'/G-expansion method [27,28], the rank analytical technique [29] and phase-plane analysis [30,31].

In this work, we use the tanh method as a useful tool for the computation of the exact travelling waves by introducing a power series in tanh function (function of hyperbolic tangent). The efficiency of the tanh method has been illustrated in [16–19] by applying it for a variety of selected equations, such as nonlinear equations of the Fischer type and the generalized Korteveg–de-Vries equation. Moreover, its modification, the tanh − coth method [19,32], is used to derive the solitons and kink solutions for some of the well-known nonlinear parabolic partial differential equations (the Newell–Whitehead, Fitz–Hugh–Nagumo and Burgers–Fisher equations). The tanh − coth method extends a set of the possible solutions and provides abundant solitons and kink solutions in addition to the existing ones. As a result, the power of the tanh method is confirmed as the most direct and effective algebraic methods [32,33] for finding the exact solutions of nonlinear differential equations.

Let us consider spatially one-dimensional equation (1.1) for the atomic density amplitude $u(x, t)$, which is evolving in time t along spatial coordinate x. Following Malfliet & Hereman [16] as well as Wazwaz [19], we introduce a new independent variable

$$\xi = \frac{x - ct}{\delta}, \tag{2.1}$$

which describes propagation of the amplitude with the velocity c and transforms the amplitude $u(x, t) \to U(\xi)$. This transformation rewrites the derivatives as follows:

$$\frac{\partial}{\partial t} = -\frac{c}{\delta}\frac{d}{d\xi}, \quad \frac{\partial^2}{\partial t^2} = \frac{c^2}{\delta^2}\frac{d^2}{d\xi^2} \quad \text{and} \quad \frac{\partial}{\partial x} = \frac{1}{\delta}\frac{d}{d\xi}, \quad \frac{\partial^2}{\partial x^2} = \frac{1}{\delta^2}\frac{d^2}{d\xi^2}. \tag{2.2}$$

Using derivatives from equation (2.2), spatially one-dimensional equation (1.1) in the new variable looks like

$$\frac{c}{\delta}\frac{dU(\xi)}{d\xi} - \tau\frac{c^2}{\delta^2}\frac{d^2U(\xi)}{d\xi^2} + \frac{1}{\delta^2}\frac{d^2U(\xi)}{d\xi^2} - K_0 U(\xi) + bU^2(\xi) - U^3(\xi) = 0. \tag{2.3}$$

To solve equation (2.3), we shall apply the tanh method [16,17], introducing the finite expansion

$$U(\xi) = S(Y) = \sum_{k=0}^{M} a_k Y^k + \sum_{k=1}^{M} b_k Y^{-k} \tag{2.4}$$

and

$$\mathbf{M} \in Z, \quad Y = \tanh(\xi). \tag{2.5}$$

Using the new variable by equation (2.5) and taking into account the derivatives $d/d\xi = (1 - Y^2)\,d/dY$, $d^2/d\xi^2 = (1 - Y^2)[-2Y\,d/dY + (1 - Y^2)\,d^2/dY^2]$, equation (2.3) is described by

$$\frac{c}{\delta}(1 - Y^2)\frac{dS}{dY} + \frac{1}{\delta^2}(1 - \tau c^2)\left\{(1 - Y^2)\left[-2Y\frac{dS}{dY} + (1 - Y^2)\frac{d^2S}{dY^2}\right]\right\}$$
$$- K_0 S + bS^2 - S^3 = 0. \tag{2.6}$$

The parameter M from equation (2.4) can be determined using the analysis given in [16,17]. Indeed, balancing the linear terms of the highest order with the highest order nonlinear terms

in equation (2.6), one can get $3M = 4 + M - 2$; therefore, $M = 1$. Balancing the linear terms of the highest order in equation (2.6), one obtains $M = 1$, so the expansion (2.4) becomes

$$S(Y) = a_0 + a_1 Y, \tag{2.7}$$

with the following derivatives:

$$S'(Y) = \sum_{k=0}^{M} (a_k Y^k)' = a_1 \quad \text{and} \quad S''(Y) = 0. \tag{2.8}$$

Now, using equations (2.7) and (2.8), we collect the coefficients of powers of Y^n in equation (2.3) as

$$\left[\frac{2}{\delta^2} (1 - \tau c^2) a_1 - a_1^3 \right] Y^3 - \left(\frac{c}{\delta} a_1 + 3 a_0 a_1^2 - b a_1^2 \right) Y^2$$

$$+ \left[\frac{2}{\delta^2} (1 - \tau c^2) a_1 - 3 a_0^2 a_1 - K_0 a_1 + 2 b a_0 a_1 \right] Y^1$$

$$+ \left(a_1 \frac{c}{\delta} - a_0^3 - a_0 K_0 + b a_0^2 \right) Y^0 = 0. \tag{2.9}$$

Equation (2.9) has a solution if the braces ahead of Y^k are placed to zero. As such, the following system of equations regarding the parameters a_k ($k = 0...M$), c and δ is obtained:

$$Y^3: \quad \frac{2}{\delta^2} (1 - \tau c^2) a_1 - a_1^3 = 0, \tag{2.10}$$

$$Y^2: \quad -\frac{c}{\delta} a_1 - 3 a_0 a_1^2 + b a_1^2 = 0, \tag{2.11}$$

$$Y^1: \quad -\frac{2}{\delta^2} (1 - \tau c^2) a_1 - 3 a_0^2 a_1 - K_0 a_1 + 2 a_0 a_1 b = 0 \tag{2.12}$$

and

$$Y^0: \quad a_1 \frac{c}{\delta} - a_0^3 - a_0 K_0 + b a_0^2 = 0. \tag{2.13}$$

The system of equations (2.10)–(2.13) has a trivial solution $a_1 = 0$ and $a_0 = (b/2) \left(1 \pm \sqrt{1 - 4K_0/b^2} \right)$ with the arbitrary values of c and δ. In this case, the amplitude has constant profile $u(x, t) = a_0$. This homogeneous solution has no interest for us because we are looking for the inhomogeneous amplitude's profiles of atomic density, which are moving through the metastable/unstable homogeneous state (liquid phase). In the case $a_1 \neq 0$, equations (2.10)–(2.13) look like

$$a_1^2 = \frac{2}{\delta^2} (1 - \tau c^2), \tag{2.14}$$

$$a_1 = \frac{c}{\delta(b - 3a_0)}, \tag{2.15}$$

$$3a_0^2 - 2a_0 b + \frac{2}{\delta^2} (1 - \tau c^2) + K_0 = 0 \tag{2.16}$$

and

$$a_0^3 - b a_0^2 + a_0 K_0 - a_1 \frac{c}{\delta} = 0. \tag{2.17}$$

Equations (2.14)–(2.17) imply several analytical constraints. First, the reality of a_1 in equation (2.14) imposes the condition: $1 - \tau c^2 > 0$, which gives an upper bound in the absolute value of the amplitude's velocity c (i.e. $|c| < 1/\sqrt{\tau} = c_{max}$ and $c_{max} \to \infty$ with $\tau \to 0$). Second, recalling that the sign of a_1 determines the polarity of the amplitudes, we may assume that, for the propagation towards the positive direction on the x-axis, $c > 0$, one finds $a_1 > 0$ for $a_0 < b/3$, and $a_1 < 0$ for $a_0 > b/3$. Respectively, if the amplitude's profile moves in the direction of negative values of x-axis, $c < 0$, one finds $a_1 > 0$ for $a_0 > b/3$ and $a_1 < 0$. Furthermore, there is no solution (at least using the tanh method) if $a_0 = b/3$. And, *third*, recall that, for $c < 0$, one has $\tanh(x - ct) = \tanh(x + |c|t) = -\tanh((-x) - |c|t)$. Hence a negative value of c is physically tantamount to transformations: space reversal, $x \to -x$; polarity reversal, $a_1 \to -a_1$; and velocity

reversal, $c \to -c = |c| > 0$. In simple terms, propagation of the amplitude's profile, $\tanh(x - ct)$), to the left is the same as propagation of the amplitude's profile, $-\tanh(x - ct)$, to the right.

Determining the parameters a_0, a_1, δ and c from equations (2.14)–(2.17) leads to the amplitude profiles (2.4) and (2.5) of the form

$$u(x,t) = a_0 + a_1 \tanh\left(\frac{x - ct}{\delta}\right). \tag{2.18}$$

Concrete values for a_0, a_1, δ and c present different types of solutions that are shown in the next two sections.

3. General set of solutions

A complete set of solutions consists of 12 decisions for the parameters K_0 and b which are defined by equations (1.2) and (1.3). This number of decisions follows from the degrees of equations (2.14)–(2.17), where equation (2.14) and equation (2.16) assume two roots for each expression (four roots in total), multiplied by three decisions from the cubic equation (2.17). These 12 decisions can be divided into three sets, each one of which contains four similar by notation type of solutions. All coefficients from equation (2.18) are obtained for the following far field boundary conditions, $\xi \to \pm\infty$: $u \equiv \mathrm{const.}$, namely for $u = 0$ or $u = \pm1$.

(a) Set of solutions 1–4

The first set of solutions can be recognized by the signs of the parameters a_1 and c. As a result, solutions 1–4 are presented in table 1, two of which are shown in figure 1.

With $b = 0$ and $K_0 = -1$, table 1 shows that $a_0 = 0$, $a_1 = \pm1$, $\delta = \mp\sqrt{2}$ and $c = 0$. In this particular case, equation (2.18) predicts stationary profiles:

$$u(x,t) = \pm \tanh\left(\mp \frac{x}{\sqrt{2}}\right). \tag{3.1}$$

This profile is consistent with the steady solution of the hyperbolic Allen–Cahn equation ($\tau \neq 0$) and the parabolic Allen–Cahn equation ($\tau = 0$), which are obtained from equation (1.1) for the above accepted parameters $b = 0$ and $K_0 = -1$.

(b) Set of solutions 5–8

The second set of solutions, consisting of solutions 5–8, has a similar structure to that of the set of solutions 1–4. To simplify the representation, we shall introduce the following notations for these solutions:

$$A_{5-8} = \left[-\left(10b^2 + 6b\sqrt{b^2 - 4K_0} + 162\tau K_0^2 - 36K_0 - 72b^2\tau K_0 + 8b^4\tau\right) \right.$$

$$\left. \times \left(8b^2 K_0 - b^4 - 6bK_0\sqrt{b^2 - 4K_0} + b^3\sqrt{b^2 - 4K_0} - 18K_0^2\right) \right]^{1/2}, \tag{3.2}$$

$$B_{5-8} = 5b^2 + 3b\sqrt{b^2 - 4K_0} + 81\tau K_0^2 - 18K_0 - 36b^2\tau K_0 + 4b^4\tau \tag{3.3}$$

and $$G_{5-8} = \sqrt{2b^2 + 2b\sqrt{b^2 - 4K_0} - 4K_0}. \tag{3.4}$$

Now, using equations (3.2)–(3.4), we rewrite solutions 5–8 in new designations:

$$\left.\begin{aligned}
a_0 &= \frac{1}{4}b + \frac{1}{4}\sqrt{b^2 - 4K_0}, \quad a_1 = \frac{1}{4}G_{5-8}, \quad \delta = \frac{2A_{5-8}}{B_{5-8}K_0}, \\
c &= -\frac{1}{4}\left(-\frac{1}{2}b + \frac{3}{2}\sqrt{b^2 - 4K_0}\right)G_{5-8}\frac{A_{5-8}}{B_{5-8}K_0},
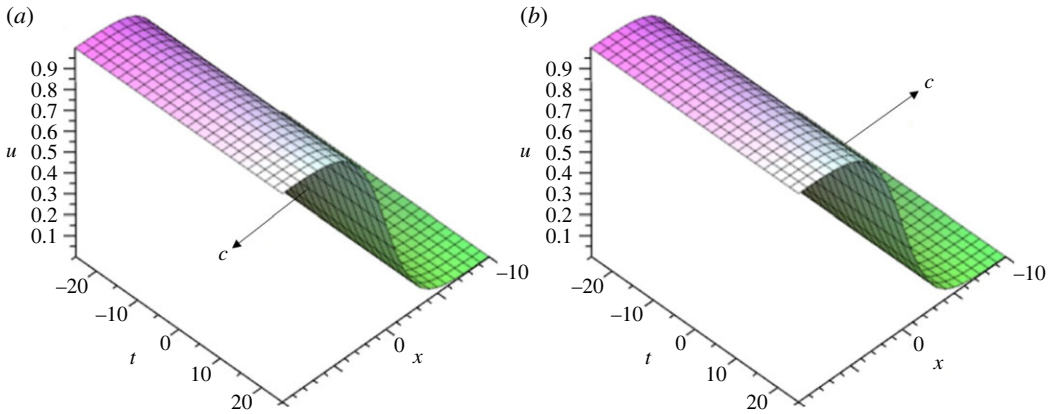\end{aligned}\right\} \tag{3.5}$$

Figure 1. u-Profiles as functions of the spatial coordinate x and the time t calculated with the usage of solutions 3 and 4 from table 1. Calculations were carried out for fixed relaxation time $\tau = 0.5$ and for the values of a_0, a_1 and δ given by $K_0 = 1$ and under the condition of $b^2 \geq 4K_0$ (table 1). (*a*) u-profile moves in the direction of the x-axis with constant positive velocity c. (*b*) u-profile moves in the direction of the x-axis with constant negative velocity c.

Table 1. First set: solutions 1–4.

values	solutions 1 and 2	solutions 3 and 4
a_0	$b/2$	$b/2$
a_1	$\pm\dfrac{1}{2}\sqrt{b^2 - 4K_0}$	$\dfrac{1}{2}\sqrt{b^2 - 4K_0}$
δ	$\dfrac{4}{\sqrt{2b^2 - 8K_0 + b^4\tau - 4b^2\tau K_0}}$	$-\dfrac{4}{\sqrt{2b^2 - 8K_0 + b^4\tau - 4b^2\tau K_0}}$
c	$\dfrac{b\sqrt{b^2 - 4K_0}}{\sqrt{2b^2 - 8K_0 + b^4\tau - 4b^2\tau K_0}}$	$\pm\dfrac{b\sqrt{b^2 - 4K_0}}{\sqrt{2b^2 - 8K_0 + b^4\tau - 4b^2\tau K_0}}$

$$a_0 = \frac{1}{4}b + \frac{1}{4}\sqrt{b^2 - 4K_0}, \quad a_1 = \frac{1}{4}G_{5-8}, \quad \delta = -\frac{2A_{5-8}}{B_{5-8}K_0}, \quad \left.\begin{array}{l}\\ \\ \end{array}\right\}$$
$$c = \frac{1}{4}\left(-\frac{1}{2}b + \frac{3}{2}\sqrt{b^2 - 4K_0}\right)G_{5-8}\frac{A_{5-8}}{B_{5-8}K_0}, \tag{3.6}$$

$$a_0 = \frac{1}{4}b + \frac{1}{4}\sqrt{b^2 - 4K_0}, \quad a_1 = -\frac{1}{4}G_{5-8}, \quad \delta = \frac{2A_{5-8}}{B_{5-8}K_0}, \quad \left.\begin{array}{l}\\ \\ \end{array}\right\}$$
$$c = \frac{1}{4}\left(-\frac{1}{2}b + \frac{3}{2}\sqrt{b^2 - 4K_0}\right)G_{5-8}\frac{A_{5-8}}{B_{5-8}K_0} \tag{3.7}$$

and
$$a_0 = \frac{1}{4}b + \frac{1}{4}\sqrt{b^2 - 4K_0}, \quad a_1 = -\frac{1}{4}G_{5-8}, \quad \delta = -\frac{2A_{5-8}}{B_{5-8}K_0}, \quad \left.\begin{array}{l}\\ \\ \end{array}\right\}$$
$$c = -\frac{1}{4}\left(-\frac{1}{2}b + \frac{3}{2}\sqrt{b^2 - 4K_0}\right)G_{5-8}\frac{A_{5-8}}{B_{5-8}K_0}. \tag{3.8}$$

(c) Set of solutions 9–12

The third set, consisting of solutions 9–12, has a similar structure to that of the sets of solutions 1–4 and solutions 5–8. Introducing the parameters

$$A_{9-12} = \left[-\left(-10b^2 + 6b\sqrt{b^2 - 4K_0} - 162\tau K_0{}^2 + 36K_0 + 72b^2\tau K_0 - 8b^4\tau \right) \right.$$
$$\left. \left(-8b^2 K_0 + b^4 - 6bK_0\sqrt{b^2 - 4K_0} + b^3\sqrt{b^2 - 4K_0} + 18K_0{}^2 \right) \right]^{1/2}, \qquad (3.9)$$

$$B_{9-12} = -5b^2 + 3b\sqrt{b^2 - 4K_0} - 81\tau K_0{}^2 + 18K_0 + 36b^2\tau K_0 - 4b^4\tau \qquad (3.10)$$

and
$$G_{9-12} = \sqrt{2b^2 - 2b\sqrt{b^2 - 4K_0} - 4K_0}, \qquad (3.11)$$

we finally rewrite parameters a_0, a_1, δ and c (given previously for solutions 5–8) as

$$\left. \begin{aligned} & a_0 = \frac{1}{4}b - \frac{1}{4}\sqrt{b^2 - 4K_0}, \quad a_1 = \frac{1}{4}G_{9-12}, \quad \delta = -\frac{2A_{9-12}}{BK_0}, \\ & c = \frac{1}{4}\left(-\frac{1}{2}b - \frac{3}{2}\sqrt{b^2 - 4K_0} \right) G_{9-12}\frac{A_{9-12}}{BK_0}, \end{aligned} \right\} \qquad (3.12)$$

$$\left. \begin{aligned} & a_0 = \frac{1}{4}b - \frac{1}{4}\sqrt{b^2 - 4K_0}, \quad a_1 = \frac{1}{4}G_{9-12}, \quad \delta = \frac{2A_{9-12}}{BK_0}, \\ & c = -\frac{1}{4}\left(-\frac{1}{2}b - \frac{3}{2}\sqrt{b^2 - 4K_0} \right) G_{9-12}\frac{A_{9-12}}{BK_0}, \end{aligned} \right\} \qquad (3.13)$$

$$\left. \begin{aligned} & a_0 = \frac{1}{4}b - \frac{1}{4}\sqrt{b^2 - 4K_0}, \quad a_1 = -\frac{1}{4}G_{9-12}, \quad \delta = -\frac{2A_{9-12}}{BK_0}, \\ & c = -\frac{1}{4}\left(-\frac{1}{2}b - \frac{3}{2}\sqrt{b^2 - 4K_0} \right) G_{9-12}\frac{A_{9-12}}{BK_0} \end{aligned} \right\} \qquad (3.14)$$

and
$$\left. \begin{aligned} & a_0 = \frac{1}{4}b - \frac{1}{4}\sqrt{b^2 - 4K_0}, \quad a_1 = -\frac{1}{4}G_{9-12}, \quad \delta = \frac{2A_{9-12}}{BK_0}, \\ & c = \frac{1}{4}\left(-\frac{1}{2}b - \frac{3}{2}\sqrt{b^2 - 4K_0} \right) G_{9-12}\frac{A_{9-12}}{BK_0}. \end{aligned} \right\} \qquad (3.15)$$

4. Set of particular solutions

For the amplitude's equation (2.3) the whole set of 12 solutions of the form of equation (2.18) is presented by the coefficients summarized in table 1, equations (3.5)–(3.8) and equations (3.12)–(3.15). Now, we compare special and particular cases of these solutions with corresponding results obtained earlier.

Using the first integral method [21], travelling wave solutions have been obtained for the hyperbolic Allen–Cahn equation [22]. This equation is consistent with equation (1.1) if $b = 0$ and $K_0 = -1$. Indeed, if we substitute these values for b and K_0 into solutions (3.5)–(3.8), then solutions of the form (2.18) correspond to those ones obtained in [22]. The graphical representation for this particular case is shown in figure 1, which gives a view for the atomic density profile that invades the homogeneous phase with positive and negative values of c. Another pair of solutions related to this particular case could be obtained for $a_0 = a_1 = \pm 0.5$. Thus, in general, we have obtained four bounded solutions, which correspond to four bounded solutions of Nizovtseva *et al.* [22]. It should be noted that in [22] other four unbounded solutions were obtained. These solutions were extracted from the general set of solutions due to its physical and mathematical insolvency, namely, due to the absence of their physical meaning and the violation of the initial statement of the mathematical problem. In this work, we do not obtain the unbounded solutions because the

tanh method states solutions (2.4)–(2.5) on the bounded set *a priori*: the solution (2.18) is always mathematically bounded.

With zero relaxation time, $\tau = 0$, the hyperbolic equation (1.1) transforms to the partial differential equation of parabolic type whose travelling-wave solution has been previously found by Wazwaz [19]. Indeed, as it follows from our solutions (3.12)–(3.15), if we use $\tau = 0$ and take into account (3.9)–(3.11), solutions of Wazwaz [19] are covered for the extended Allen–Cahn equation.

In general, we have obtained travelling wave solutions represented by hyperbolic tanh functions (2.18), which confirms the correctness of the particular solutions for the dynamical problem of fast diffuse interfaces [34].

5. Travelling waves in amplitudes of phase-field crystals

To demonstrate the applicability of the general solution (2.18) together with its set of concrete and particular solutions summarized in §§3 and 4, let us consider the dynamics of the diffuse crystal–liquid interface propagation as described by the PFC model [4]. In this model, investigation of the dynamics of periodic pattern propagation plays an important role [4]. Figure 2 presents a scheme for spatial distribution of the atomic density field near a solid–liquid interface, where peaks correspond to average atomic positions. The envelope of these peaks is described by the PFC amplitude's equation and is consistent with the phase-field profile shown in figure 1. The interface width W in figure 2 represents the transition region between the atomically homogeneous state (liquid phase) and periodic states (crystal phase), i.e. the diffuse crystal–liquid interface.

(a) Analytical solution

The PFC amplitude's equations were derived in [6–8]. In this work, we use the PFC amplitude's equation in accordance with the work of Humadi *et al.* [35]:

$$\tau^2 c^2 \frac{\mathrm{d}^2 u}{\mathrm{d}\xi^2} - c\frac{\mathrm{d}u}{\mathrm{d}\xi} = W^2(\hat{n})\frac{\mathrm{d}^2 u}{\mathrm{d}\xi^2} - \frac{\mathrm{d}f}{\mathrm{d}u}, \tag{5.1}$$

where u is the amplitude's profile, τ is the relaxation time of the rate $\partial u/\partial t$ of change of the amplitude u (i.e. $\partial u/\partial t$ is the gradient flow) and $W(\hat{n}) = B_0^s \sum_i \hat{n} \cdot \mathbf{G}_i$ is the measure of the width of the diffuse transitive layer having the local normal vector $\hat{n}$ and the reciprocal lattice vector G_{hkl} with Miller indexes h, k and l.

In equation (5.1), the free energy density $f(u)$ is expressed by

$$f(\Delta B_0, u) = f_0(\Delta B_0^{\mathrm{eq}}, u) + \frac{a}{2}u^2 - \frac{b}{3}u^3 + \frac{h}{4}u^4, \tag{5.2}$$

where

$$a = 6(\Delta B_0 + B_2^l c_c^2), \quad b = 12r \quad \text{and} \quad h = 90\tilde{v}. \tag{5.3}$$

Here, c_c is the concentration of a solute in a chemically binary system.[1] Upper indexes l and s are related to the liquid and solid phases, respectively. Lower indexes 0 and 2 are related to the coefficients of the zero and second order; and r and $\tilde{v}$ are the coefficients corresponding to u^3 and u^4, respectively. The driving force, $\Delta B_0 = B_0^l - B_0^x$, is the difference between the dimensionless liquid compressibility B_0^l and the dimensionless elastic module B_0^x. In equilibrium at $\Delta B_0 = \Delta B_0^{\mathrm{eq}}$, the elasticity compensates the compressibility, that is $B_0^l = B_0^x$.

The free energy (5.2) has the form of the Landau–de Gennes potential, which has been used in the theory of weak crystallization [36] as well as in the PFC model [4]. This potential describes various states, which exist for possible transformations from metastable to stable or from unstable to stable states. In the present derivation, we shall use the configuration of states consistently with the transition from metastable liquid to stable crystal such that $\Delta B_0 > 0$ (see, for details, [8]).

---

[1]Humadi *et al.* [35] derived the amplitude's equation for u together with an additional equation for the concentration c_c. They have solved this system of two equations under some approximations analytically and numerically. For the sake of simplicity, in this work, we assume the constant concentration, $c_c \equiv \mathrm{const.}$, and find an exact analytical solution of equation (5.1).
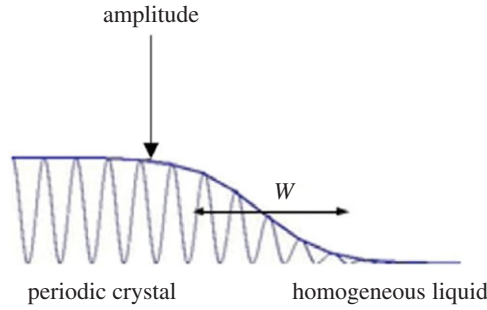
Figure 2. Diffuse front of a periodic crystal invading homogeneous liquid. Crystal and liquid are divided by the diffuse transitive layer of the width W. The amplitude represents the envelope of atomic density peaks.

Finally, the free energy (5.1) corresponds to equation (2.3), and the free energy density (5.2) of Humadi *et al.* [35] is equivalent to equation (1.4) for our general derivation of the equation set.

Introducing normalized velocity $\tilde{c} = c/W$ and correlation length $\tilde{\xi} = \xi/W$, equation (5.1) transforms to

$$(1 - \tau^2 \tilde{c}^2)\frac{d^2 u}{d\tilde{\xi}^2} + \tilde{c}\frac{du}{d\tilde{\xi}} - au + bu^2 - hu^3 = 0. \tag{5.4}$$

We search for a solution of equation (5.4) for the condition $\tau^2 \tilde{c}^2 < 1$ (i.e. for $\tau < \tilde{c}^{-1}$). This condition means that the interface velocity $\tilde{c}$ cannot overcome and be larger than the maximum speed of disturbance propagation in the field of order parameter u [11,34].

Using the general solution (2.18), we find the particular solution of (5.4) in the following form:

$$u(\tilde{\xi}) = A\left[1 - \tanh\left(\frac{\tilde{\xi}}{\delta}\right)\right], \tag{5.5}$$

with A the amplitude factor and δ the correlation length. In this case, the derivatives are

$$\frac{du}{d\tilde{\xi}} = \frac{u}{\delta}\left(\frac{u}{A} - 2\right), \quad \frac{d^2 u}{d\tilde{\xi}^2} = \frac{2u}{\delta^2}\left(\frac{u}{A} - 1\right)\left(\frac{u}{A} - 2\right). \tag{5.6}$$

Then, equation (5.4) can be rewritten as

$$\frac{2u}{\delta^2}\left(\frac{u}{A} - 1\right)\left(\frac{u}{A} - 2\right)(1 - \tau^2 \tilde{c}^2) + \frac{u\tilde{c}}{\delta}\left(\frac{u}{A} - 2\right) - au + bu^2 - hu^3 = 0. \tag{5.7}$$

Equation (5.7) immediately gives the solution $u = 0$, which describes the homogeneous state in a whole domain and has no interest for us. Then, opening the brackets and combining the u-terms with the same degree in equation (5.7), we obtain the following system of three equations:

$$\left.\begin{array}{l} u^2: \dfrac{2}{A^2 \delta^2}(1 - \tau^2 \tilde{c}^2) - h = 0, \\[2mm] u^1: -\dfrac{6}{A\delta^2}(1 - \tau^2 \tilde{c}^2) + \dfrac{\tilde{c}}{A\delta} + b = 0 \\[2mm] u^0: \dfrac{4}{\delta^2}(1 - \tau^2 \tilde{c}^2) - \dfrac{2\tilde{c}}{\delta} - a = 0, \end{array}\right\} \tag{5.8}$$

and

with three unknown parameters A, δ and $\tilde{c}$. As the result, the system of equations (5.8) gives

— the solution for the positive amplitude factor A,

$$A = \frac{1}{4h}\left(b + \sqrt{b^2 - 4ah}\right); \tag{5.9}$$

— the solution for the diffuse interface velocity $\tilde{c}$,

$$\tilde{c} = \frac{\tilde{c}_{\mathrm{m}}}{\sqrt{1 + \tau^2 \tilde{c}_{\mathrm{m}}^2}}, \tag{5.10}$$

with its maximum value $\tilde{c}_{\mathrm{m}}$,

$$\tilde{c}_{\mathrm{m}} = \frac{\sqrt{2h}}{4} \left[3\sqrt{b^2 - 4ah} - \left(\frac{4}{h} + 3 \right) b \right]; \tag{5.11}$$

— the solution for the correlation length δ,

$$\delta = \frac{4\sqrt{2h(1 - \tau^2 \tilde{c}^2)}}{b + \sqrt{b^2 - 4ah}} = \frac{4\sqrt{2h}}{(b + \sqrt{b^2 - 4ah})\sqrt{1 + \tau^2 \tilde{c}_{\mathrm{m}}^2}}. \tag{5.12}$$

In equations (5.9)–(5.12) we have the condition $|b| > 2\sqrt{ah}$.

Finally, for the analysis of the dynamics of crystal front invading liquid by equations (5.5) and (5.9)–(5.12), we obtain now the driving force ΔB_0 relative to its equilibrium value ΔB_0^{eq} which is chosen as a reference. From equation (5.2) it follows that the equilibrium state, having equal energy states, is defined by the equality $f(\Delta B_0, u) = f_0(\Delta B_0^{\mathrm{eq}}, u) \equiv 0$. From this immediately follows the trivial solution $u_1 = 0$, which again is of no interest to us as the homogeneous solution for a whole domain. For the other solutions under the condition of equal energy states, one can find

$$u_{2,3} = \frac{2b}{3h} \pm \sqrt{\frac{4b^2}{9h^2} - \frac{2a}{h}}. \tag{5.13}$$

In the equilibrium, $u_2 = u_3$, the condition

$$\frac{4b^2}{9h^2} = \frac{2a}{h} \tag{5.14}$$

should be satisfied. Using the parameter a from equation (5.3), the equilibrium value for the driving force is obtained as

$$\Delta B_0^{\mathrm{eq}} = \frac{b^2}{27h} - B_2^{\mathrm{l}} c^2. \tag{5.15}$$

As the result, for the further analysis and graphical interpretation of equations (5.5) and (5.9)–(5.12) we use the normalized driving force $\Delta \tilde{B}_0$:

$$\Delta \tilde{B}_0 = \frac{\Delta B_0^{\mathrm{eq}} - \Delta B}{\Delta B_0^{\mathrm{eq}}}. \tag{5.16}$$

(b) Numerical representation of analytical solutions

(i) Calculations

The amplitude front, i.e. the crystal–liquid boundary layer having a step-like profile, is a crystallization front invading the metastable liquid (figure 2). The travelling wave (5.5) serves to analyse the dynamics of the amplitude front. The profile of the amplitude front can be determined by three variables: (i) the amplitude factor A from equation (5.9), (ii) the velocity $\tilde{c}$ from equations (5.10) and (5.11) with which the front moves, and (iii) the correlation length δ from equation (5.12). These variables depend on the driving force $\Delta \tilde{B}_0$ given by equations (5.15) and (5.16) through the parameter a given by equation (5.3). In addition, the velocity $\tilde{c}$ and correlation length δ depend on the relaxation time τ of the gradient flow $\partial u / \partial t$. Using calculation results, we show how the driving force and the relaxation parameter τ influence the profile of the amplitude density u, amplitude factor A, front velocity $\tilde{c}$ and correlation length δ. The model parameters are used for the calculations as follows: $B_2^{\mathrm{l}} = -1.8$, $c_{\mathrm{c}} = 0.1$, $r = 4.25 \times 10^{-10}$, $\tilde{v} = 0.012$ and $\tau^2 = 0.1$. Note that the relaxation time τ has been taken as a constant value only
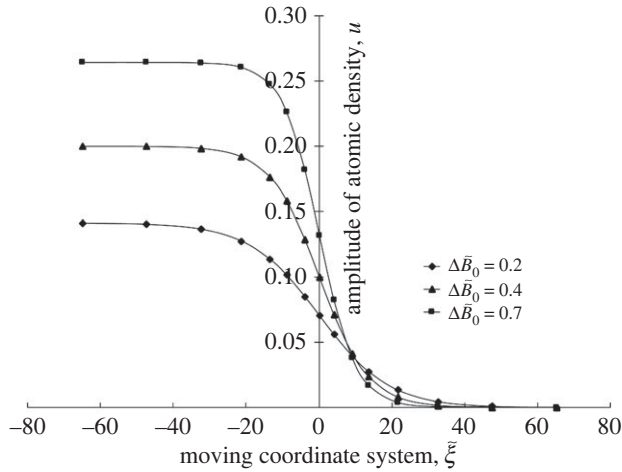
Figure 3. Amplitude of the atomic density as a function of the moving coordinate system according to equations (5.5) and (5.9)–(5.12).
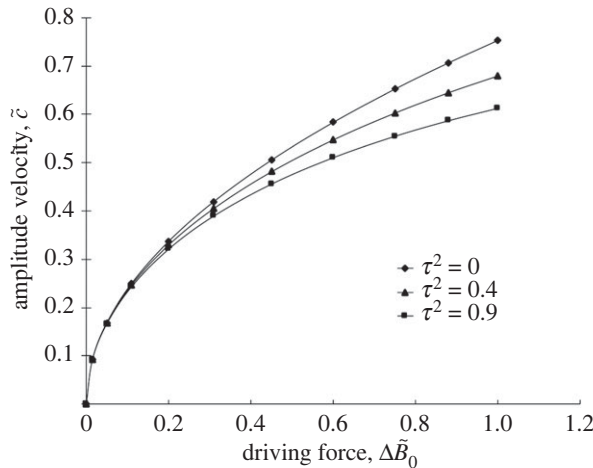

Figure 4. Amplitude's velocity as a function of the driving force according to equations (5.10) and (5.11).

for calculations of the amplitude density u and amplitude factor A. The front velocity $\tilde{c}$ and correlation length δ are shown for different values of τ (see next section).

(ii) Influence of driving force and relaxation time

The influence of the driving force $\Delta\tilde{B}_0$ on the phase-field profile is shown in figure 3, where the solution equation (5.5) with equations (5.9)–(5.12) exhibits a dynamical step-like profile for the atomic density amplitude. It is clearly seen from figure 3 that the increase of $\Delta\tilde{B}_0$ makes the step-like profile within the diffuse interface between the crystal and the liquid steeper. Therefore, the gradient of atomic density has maximal values at a higher driving force in the transition from the diffuse to sharp interface.

Figure 4 shows nonlinear dependence of the velocity for the amplitude's profile. Such dependence is consistent with the data of numerical molecular dynamics simulation [37] and recent advancements on kinetics of fast interfaces [38]. As also follows from figure 4, the amplitude velocity $\tilde{c}$ depends on the values of relaxation time τ. The difference between velocities
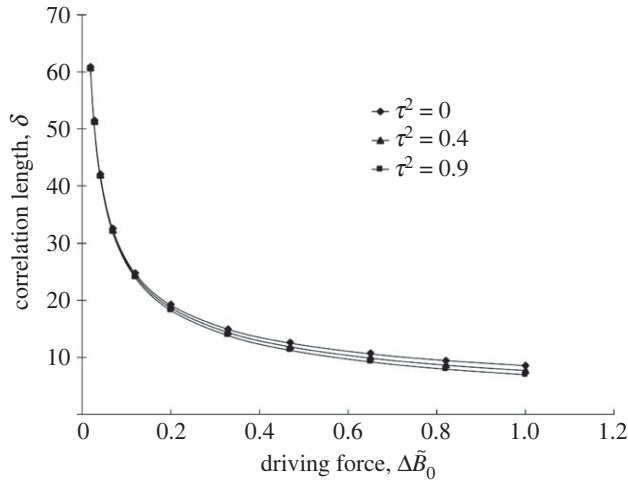
Figure 5. Correlation length as a function of the driving force according to equation (5.12).

for different τ occurs, however, at moderate and large values of driving forces, namely, at $\Delta\tilde{B}_0 > 0.2$. At small $\Delta\tilde{B}_0$, the influence of relaxation time τ is negligible. Such dependence exists due to the fact that the time τ influences the relaxation of fast variable—gradient flow, $\partial u/\partial t$— the variable which plays an essential role far from the equilibrium [11]. A general tendency is that a longer relaxation time τ makes the velocity increase slower. Indeed, the dynamics by the parabolic Allen–Cahn equation (see equation (1.1) with $\tau = 0$) is defined by the relaxation of the order parameter u only. The dynamics by the hyperbolic Allen–Cahn equation (1.1) is already defined by the relaxation of the order parameter u and by the gradient flow $\partial u/\partial t$. As a result, in comparison with the parabolic dynamics, the additional relaxation in the hyperbolic dynamics makes the velocity $\tilde{c}$ smaller with the increase in relaxation time τ for a given $\Delta\tilde{B}_0$.

Dependence of correlation length δ on the driving force and relaxation time is shown in figure 5. The drastic change in δ occurs at smaller values of the driving force, namely, at $\Delta\tilde{B}_0 < 0.2$. Gradual decrease of δ to its minimal values occurs at moderate and large values of driving forces, i.e. at $\Delta\tilde{B}_0 > 0$, showing that far from the equilibrium the interface becomes steeper, which directly follows from equation (5.12). It can also be seen from figure 5 that the larger relaxation time τ reduces the correlation length of the atomic density amplitude for $\Delta\tilde{B}_0 > 0.2$. Therefore, longer relaxation time τ at large driving force makes the interface steeper as a result of essential deviation from the equilibrium.

6. Conclusion

The propagation of amplitudes of the atomic density of crystals which invade a homogeneous liquid state has been analysed. Using the PFC model [4], amplitude equation (1.1) for the atomic density has been solved by application of the tanh method [16–19,32,33].

A set of travelling wave solutions obtained on the basis of the general solution (2.18) are described by tanh functions. This confirms the correctness of the previously used particular solutions [34] used for fast transformations in materials. The set of solutions includes travelling waves previously found for (i) the extended parabolic Allen–Cahn equation [17] and (ii) the hyperbolic Allen–Cahn equation with a free energy of a double-well form which describes transitions from an unstable state [22].

The general tanh solution is analysed within a specific task of a crystal front invading metastable liquid. We have found spatial profiles of atomic density amplitude u, amplitude velocity $\tilde{c}$ and correlation length δ as the functions in driving force $\Delta\tilde{B}_0$. We have shown that

amplitude of atomic density decreases, velocity increases and correlation length drastically decreases with the increase of the driving force. It is also shown that a longer relaxation of the gradient flow makes the velocity increase with a slower driving force. Such results well agree with the particular travelling-wave solutions [8] and, therefore, solutions (5.5) and (5.9)–(5.12), which are graphically shown in figures 3–5, can be used as benchmarks for various numerical solutions of the PFC equation. Because periodic density fields play a crucial role in the formation of crystal lattices and dendrites [39], the present travelling-wave solutions can also be useful for the estimations of interface dynamics of dendritic patterns.

Appendix A. A couple remarks on amplitude equations

Amplitude equations (AEq) [7,8] of the regular PFC equation provide a description of envelopes of maxima of atomic density distribution in crystals having different symmetry (triangular, hexagonal, cubic symmetry, etc.). They appear as a result of a coarse-graining procedure providing transition from the nano-length periodic pattern (described by the regular PFC equation of the sixth order in space) to a monotonically smoothing mesoscale pattern (described by the AEq which already has the second order in space). This procedure is based on the renormalization group theory and was developed analytically by Goldenfeld *et al.* [5,6]. As a result of this procedure, one can formulate a physical meaning of the classical phase field as a non-conserved order parameter: the phase field is a smooth envelope of the atomic density maxima of a given crystalline symmetry. In this sense, properties of the phase field can be measured (in the form of its mobility, gradient factor and relaxation time) in natural or computational experiments.

Shiwa [40] established a discussion about the correctness of the Goldenfeld *et al.* analysis [5,6] applied to the PFC equation for obtaining the respective AEq. First, Shiwa has found a small analytical mistake in the AGD analysis, which does not influence the final result for AEq [41]. Second, Shiwa stressed the fact that the ADG analysis fails in the description of mode coupling. More specifically, because the PFC equation describes conserved dynamics, the amplitude of slow neutral modes at zero wavenumber should be coupled with the modes at the critical wavenumber behind which a homogeneous state becomes unstable. This second issue of zeroth mode for conserved dynamics has also been successfully resolved [42] in obtaining the AEq of the PFC equation.

For practical use of AEqs, it is important to know what they are missing compared with the regular PFC equation. In addition to losing mode coupling [40,42], the other problem is the lack of barriers between boundaries [43]. AEqs are also missing instantaneous mechanical equilibrium (as is the full PFC equation) [44]. To avoid these inconsistences arising in the transition from the regular PFC equation to its AEqs, a more complete approach up to all orders of multiple scale expansion can be used (see Sect. III of Huang *et al.* [45]).

References

1. Elder KR, Grant M. 2004 Modeling elastic and plastic deformations in nonequilibrium processing using phase field crystals. *Phys. Rev. E* **70**, 051605. (doi:10.1103/PhysRevE.70.051605)
2. Elder KR, Provatas N, Berry J, Stefanovich P, Grant M. 2007 Phase-field crystal modeling and classical density functional theory of freezing. *Phys. Rev. B* **75**, 064107. (doi:10.1103/PhysRevB.75.064107)

3. Elder KR, Rossi G, Kanerva P, Sanches F, Ying S-C, Granato E, Achim CV, Ala-Nissila T. 2012 Patterning of heteroepitaxial overlayers from nano to micron scales. *Phys. Rev. Lett.* **108**, 226102. (doi:10.1103/physrevlett.108.226102)
4. Provatas N, Elder K 2010 *Phase-field methods in materials science and engineering*. Weinheim, Germany: Wiley-VCH.
5. Goldenfeld N, Athreya BP, Danzig JA. 2005 Renormalization group approach to multiscale simulation of polycrystalline materials using the phase field crystal model. *Phys. Rev. E* **72**, 020601(R). (doi:10.1103/PhysRevE.72.020601)
6. Athreya BP, Goldenfeld N, Danzig JA. 2006 Renormalization-group theory for the phase-field crystal equation. *Phys. Rev. E* **74**, 011601. (doi:10.1103/PhysRevE.74.011601)
7. Elder KR, Huang Zh-F, Provatas N. 2010 Amplitude expansion of the binary phase-field-crystal model. *Phys. Rev. E* **81**, 011602. (doi:10.1103/PhysRevE.81.011602)
8. Galenko PK, Sanches FI, Elder KR. 2015 Traveling wave profiles for a crystaline front invading liquid states. *Phys. D* **308**, 1–10. (doi:10.1016/j.physd.2015.06.002)
9. Allen SM, Cahn JW. 1979 A microscopic theory for antiphase boundary motion and its application to antiphase domain coarsening. *Acta Metall.* **27**, 1085–1095. (doi:10.1016/0001-6160(79)90196-2)
10. Van Saarloos W. 2003 Front propagation into unstable states. *Phys. Rep.* **386**, 29–222. (doi:10.1016/j.physrep.2003.08.001)
11. Galenko P, Jou D. 2005 Diffuse-interface model for rapid phase transformations in nonequilibrium systems. *Phys. Rev. E* **71**, 046125. (doi:10.1103/PhysRevE.71.046125)
12. Galenko P, Danilov D, Lebedev V. 2009 Phase-field-crystal and Swift-Hohenberg equations with fast dynamics. *Phys. Rev. E* **75**, 051110. (doi:10.1103/PhysRevE.79.051110)
13. Galenko PK, Herlach DM. 2006 Diffusionless crystal growth in rapidly solidifying eutectic systems. *Phys. Rev. Lett.* **96**, 150602. (doi:10.1103/PhysRevLett.96.150602)
14. Yang Y, Humadi H, Buta D, Laird BB, Sun D, Hoyt JJ, Asta M. 2011 Atomistic simulations of nonequilibrium crystal-growth kinetics from alloy melts. *Phys. Rev. Lett.* **107**, 025505. (doi:10.1103/PhysRevLett.107.025505)
15. Jou D, Galenko PK. 2013 Coarse graining for the phase-field model of fast phase transitions. *Phys. Rev. E* **88**, 042151. (doi:10.1103/PhysRevE.88.042151)
16. Malfliet W, Hereman W. 1996 The tanh method: I. Exact solutions of nonlinear evolution and wave equations. *Phys. Scr.* **54**, 563–568. (doi:10.1088/0031-8949/54/6/003)
17. Wazwaz A-M. 2004 The tanh method for travelling wave solutions of nonlinear equations. *Appl. Math. Comput.* **154**, 713–723. (doi:10.1016/S0096-3003(03)00745-8)
18. Fan E, Hon YC. 2002 Generalized tanh method extended to special types of nonlinear equations. *Z. Naturforsch.* **57**, 692–700. (doi:10.1515/zna-2002-0809)
19. Wazwaz A-M. 2007 The tanh-coth method for solitons and kink solutions for nonlinear parabolic equations. *Appl. Math. Comput.* **188**, 1467–1475. (doi:10.1016/j.amc.2006.11.013)
20. Kourakis I, Sultana S, Verheest F. 2012 Note on the single-shock solutions of the Korteweg-de Vries-Burgers equation. *Astrophys. Space Sci.* **338**, 245–249. (doi:10.1007/s10509-011-0958-5)
21. Feng Zh. 2002 The first-integral method to study the Burgers-Korteweg de Vries equation. *J. Phys. A: Math. Gen.* **35**, 343–349. (doi:10.1088/0305-4470/35/2/312)
22. Nizovtseva IG, Galenko PK, Alexandrov DV. 2016 The hyperbolic Allen-Cahn equation: exact solutions. *J. Phys. A: Math. Theor.* **49**, 435201. (doi:10.1088/1751-8113/49/43/435201)
23. Lu B, Zhang HQ, Xie FD. 2010 Traveling wave solutions of nonlinear partial differential equations by using the first integral method. *Appl. Math. Comput.* **216**, 1329–1336. (doi:10.1016/j.amc.2010.02.028)
24. Feng Zh, Wang X. 2003 The first integral method to the two-dimensional Burgers–Korteweg-de Vries equation. *Phys. Lett. A* **308**, 173–178. (doi:10.1016/S0375-9601(03)00016-1)
25. Fan E. 2002 Multiple travelling wave solutions of nonlinear evolution equations using a unified algebraic method. *J. Phys. A: Math. Gen.* **35**, 6853–6872. (doi:10.1088/0305-4470/35/32/306)
26. Kudryashov NA. 2009 Seven common errors in finding exact solutions of nonlinear differential equations. *Commun. Nonlinear Sci. Numer. Simulat.* **14**, 3507–3529. (doi:10.1016/j.cnsns.2009.01.023)

27. Kim H, Sakthivel R. 2010 Travelling wave solutions for time-delayed nonlinear evolution equations. *Appl. Math. Lett.* **23**, 527–532. (doi:10.1016/j.aml.2010.01.005)
28. Feng X. 2000 Exploratory approach to explicit solution of nonlinear evolution equations. *Int. J. Theor. Phys.* **39**, 207–222. (doi:10.1023/A:1003615705115)
29. Hu J, Zhang H. 2001 A new method for finding exact traveling wave solutions to nonlinear partial differential equations. *Phys. Lett. A* **286**, 175–179. (doi:10.1016/S0375-9601(01)00291-2)
30. Rehman T, Gambino G, Choudhury SR. 2013 Smooth and non-smooth traveling wave solutions of some generalized Camassa-Holm equations. *Commun. Nonlinear Sci. Numer. Simulat.* **19**, 1746–1769. (doi:10.1016/j.cnsns.2013.10.029)
31. Malfliet W. 1992 Solitary wave solutions of nonlinear wave equations. *Am. J. Phys.* **60**, 650–654. (doi:10.1119/1.17120)
32. Wazwaz A-M. 2008 The extended tanh method for new compact and noncompact solutions for the KP-BBM and the ZK-BBM equations. *Chaos Solitons Fractals* **38**, 1505–1516. (doi:10.1016/j.chaos.2007.01.135)
33. Khater AH, Malfliet W, Callebaut DK, Kamel ES. 2002 The tanh method, a simple transformation and exact analytical solutions for nonlinear reaction-diffusion equations. *Chaos Solitons Fractals* **14**, 513–522. (doi:10.1016/S0960-0779(01)00247-8)
34. Galenko PK, Abramova EV, Jou D, Danilov DA, Lebedev VG, Herlach DM. 2011 Solute trapping in rapid solidification of a binary dilute system: a phase-field study. *Phys. Rev. E* **84**, 041143. (doi:10.1103/PhysRevE.84.041143)
35. Humadi H, Hoyt JJ, Provatas N. 2016 Microscopic treatment of solute trapping and drag. *Phys. Rev. E* **93**, 010801. (doi:10.1103/PhysRevE.93.010801)
36. Kats EI, Lebedev VV, Muratov AR. 1993 Weak crystallization theory. *Phys. Rep.* **228**, 1–91. (doi:10.1016/0370-1573(93)90119-X)
37. Hoyt JJ, Sadigh B, Asta M, Foiles SM. 1999 Kinetic phase field parameters for the Cu-Ni system derived from atomistic computations. *Acta Mater.* **47**, 3181–3187. (doi:10.1016/S1359-6454(99)00189-5)
38. Salhoumi A, Galenko PK. 2017 Analysis of interface kinetics: solutions of the Gibbs-Thomson-type equation and of the kinetic rate theory. *IOP Conf. Series: Mater. Sci. Eng.* **192**, 012014. (doi:10.1088/1757-899X/192/1/012014)
39. Provatas N, Dantzig JA, Athreya B, Chan P, Stefanovic P, Goldenfeld N, Elder KR. 2007 Using the phase-field crystal method in the multi-scale modeling of microstructure evolution. *JOM* **59**, 83–90. (doi:10.1007/s11837-007-0095-3)
40. Shiwa Y. 2009 Comment on 'Renormalization-group theory for the phase-field crystal equation'. *Phys. Rev. E* **79**, 013601. (doi:10.1103/PhysRevE.79.013601)
41. Goldenfeld N, Athreya BP, Dantzig JA. 2009 Reply to 'Comment on "Renormalization-group theory for the phase-field crystal equation"'. *Phys. Rev. E* **79**, 013602. (doi:10.1103/PhysRevE.79.013602)
42. Yeon D-H, Huang Zh-H, Elder KR, Thornton K. 2010 Density-amplitude formulation of the phase-field crystal model for two-phase coexistence in two and three dimensions. *Philos. Mag.* **90**, 237–263. (doi:10.1080/14786430903164572)
43. Huang Zh-F. 2016 Scaling of alloy interfacial properties under compositional strain. *Phys. Rev. E* **93**, 022803. (doi: 10.1103/PhysRevE.93.022803)
44. Heinonen V, Achim CV, Elder KR, Buyukdagli S, Ala-Nissila T. 2014 Phase-field-crystal models and mechanical equilibrium. *Phys. Rev. E* **89**, 032411. (doi:10.1103/PhysRevE.89.032411)
45. Huang Zh-F, Elder KR, Provatas N. 2010 Phase-field-crystal dynamics for binary systems: derivation from dynamical density functional theory, amplitude equation formalism, and applications to alloy heterostructures. *Phys. Rev. E* **82**, 021605. (doi:10.1103/PhysRevE.82.021605)